Generalized Robust MTL Semantics for Problems in Cardiac Electrophysiology

Houssam Abbas and Rahul Mangharam

***Abstract*— Robustness-Guided Falsification (RGF) is an efficient testing technique that tries to find a system execution that violates some formal specification, by minimizing the *robustness* of the specification over the set of initial conditions of the system. Robustness uses an underlying distance function on the space of system executions. As RGF is applied to new fields like medicine, it is essential to determine whether our distances still capture the domain expert's intuition of which executions are similar and which are not. Motivated by the problem of testing the algorithms of cardiac defibrillators implanted in millions of patients worldwide, this work develops a (pseudo-)distance function, called *conformance*, over the space of cardiac signals. By using it to distinguish between fatal and non-fatal arrhythmias obtained from real patients, it is demonstrated that conformance measures the meaningful distance between cardiac signals much better than distances used in medical devices today. Next, conformance is used to re-define the robustness degrees of Metric Temporal Logic (MTL), and it is shown that conformance-based robust semantics of MTL can bound the (conformance-based) robustness degree, thus enabling a *principled* application of RGF to problems in the cardiac domain, *using the appropriate distance notion*. Using existing robust semantics based on sup norm can yield incorrect conclusions, with potentially severe consequences to patients.**

I. Introduction

When a system's performance is evaluated quantitatively, it is almost always necessary to measure the distance, or dissimilarity, between two different executions of the system[1]. For example, various quantitative semantics for Metric and Signal Temporal Logic (MTL/STL) use, as a basic construct, a metric over the signal space. The most basic requirement from a distance function d is that if $d(x, y) > d(x, z)$ for signals x, y, z, then this correlates positively with a domain expert's judgement that signal x is more similar to z than it is to y. As we seek to apply formal and quantitative methods to new disciplines that are ever further from the originating disciplines of these methods, it is essential that we revisit fundamental constructs, like distance between signals, to guarantee that they still capture the domain expert's judgment. If they do not, then when system performance is optimized, the optimization might fail to converge, or worse, it might converge to a *wrong* optimizer.

This work defines an appropriate distance function, and derives its consequences for robust semantics, in the field of cardiac electrophysiology. This is the branch of medicine that treats disturbances in the electrical activity of the human heart leading to Sudden Cardiac Arrest, the leading cause of death worldwide. Our overall objective is to apply robustness-guided falsification [20] to the task of finding fatal rhythms, and the cardiac conditions that produce them. The basic object in this domain is the *electrogram signal*, the voltage signal generated by the heart as it beats. To accomplish this overall objective, *this work focuses on defining the appropriate distance between electrograms, and defining the corresponding notion of robustness and establishing its properties.* We introduce conformance (Section II) and demonstrate, by testing on real patient data, that it is a superior measure of distance between electrograms than distances currently used in cardiac defibrillators (Section III). This result is also of independent interest, as conformance can be used in defibrillators to reduce the risk of inappropriate high-energy electric shocks being delivered to the patient [1].

We then re-derive the (temporal and spatial) robust semantics of MTL based on conformance, rather than the sup norm (Section IV). It is shown that even though conformance is not a metric, the conformance-based semantics approximate the (conformance-based) robustness degree, thus enabling the usage of successful robustness-guided falsification methods to electrophysiology problems. This is important because, despite recent progress [2], realistic heart models are still too complex for exhaustive verification, leaving falsification and testing as the only avenues for device verification. This result is also of independent and general interest, since it demonstrates that the robustness of MTL formulas is remarkably resilient to generic bounded measurement errors over the signals. Two examples illustrate these results (Section V).

II. Evaluating distance measures on patient data

An intracardiac *electrogram (EGM) signal* is the voltage signal generated by the heart as it beats, measured by a lead implanted in the cardiac muscle. It is composed of a sequence of *depolarizations*, as shown in Fig. 1 (a). Electrograms are noisy, non-parametric and highly variable across patients and within a patient over time. We will first describe the proposed distance over EGM space, then establish that it is more suitable for the task of finding fatal arrhythmias.

Notation. Let $\mathbb{N}$ be the set of non-negative integers, $\mathbb{R}$ be the set of real numbers, $\mathbb{R}_+ = [0, \infty)$. The Euclidian norm is denoted by $|\cdot|$, in a vector space that is clear from the context. Given a real-valued function f defined on some set S, by convention, $\inf_{s\in\emptyset} f(s) = \infty$ and $\sup_{s\in\emptyset} f(s) = -\infty$. Given two sets, A and B, A^B is the set of all functions from B to A. A *time domain* is either a real interval (e.g., $\mathbb{T} = [0, 5)$), an integer interval (e.g., $\mathbb{T} = \{0, \dots, 5\}$) or a compact hybrid time domain ($\mathbb{T} = \cup_{j=0}^{J}[t_j, t_{j+1}] \times \{j\} \subset \mathbb{R}_+ \times \mathbb{N}$) [23]. Let $X \subset \mathbb{R}^n$ be the bounded state-space. A

[1]Throughout this paper, 'distance' is used colloquially, and does not necessarily refer to the mathematical notion of distance. The word 'metric' is used for the latter.

signal is a function $\mathbf{x} : \mathbb{T} \to X$. The value of $\mathbf{x}$ at time t is denoted by x_t. The *sup norm* between signals $\mathbf{x}$ and $\mathbf{y}$ with a common domain $\mathbb{T}$ is $d_\infty(\mathbf{x}, \mathbf{y}) := \sup_{t\in\mathbb{T}} |x_t - y_t|$. We write dom$\mathbf{x}$ for the domain of $\mathbf{x}$. Given two reals a and b, $a \sqcup b$ is their maximum and $a \sqcap b$ is their minimum.

A. Conformance as a distance measure

The proposed distance, introduced in [4] for discrete-time signals, is now defined.

Definition II.1. *Given two signals* $\mathbf{x}$ *and* $\mathbf{y}$ *in* $X^{\mathbb{T}}$, $t \in \mathbb{T}$, *and given a positive real* $\tau > 0$, *the* τ-degree of conformance between $\mathbf{x}$ and $\mathbf{y}$, $\rho_\tau(\mathbf{x}, \mathbf{y})$, *is given by:*

$$\begin{aligned} \overrightarrow{d}_\tau(\mathbf{x}, \mathbf{y}, t) &:= \inf_{s\in\mathbb{T}:|t-s|<\tau} |x_t - y_s|, \\ d_\tau(\mathbf{x}, \mathbf{y}, t) &:= \overrightarrow{d}_\tau(\mathbf{x}, \mathbf{y}, t) \sqcup \overrightarrow{d}_\tau(\mathbf{y}, \mathbf{x}, t) \\ \rho_\tau(\mathbf{x}, \mathbf{y}) &:= \sup_{t\in\mathbb{T}} d_\tau(\mathbf{x}, \mathbf{y}, t) \end{aligned} \tag{1}$$

In words, function $\overrightarrow{d}_\tau$ matches each point of $\mathbf{x}$ with the nearest point on $\mathbf{y}$ *that is within some* τ *of it*. By contrast, the sup and L_p norms, both commonly used, only measure the distance at the same point in time. This is inappropriate in many scenarios where the signals are not sampled exactly at the same time, or when one signal has a (possibly variable) delay relative to the other, or noise is present. The price we pay for the generality provided by ρ_τ is that it does not separate points (i.e., we can have $\rho_\tau(\mathbf{x}, \mathbf{y}) = 0$ but $\mathbf{x} \neq \mathbf{y}$) and does not respect the triangle inequality.

B. Morphology discriminators in ICDs

To establish conformance as a suitable distance measure over EGM space, we compare its success rate in discriminating between two classes of cardiac rhythms to that of two other distances used in Implantable Cardioverter Defibrillators (ICDs) today [17]. A word about ICDs is first in order. An ICD is a life-saving cardiac device, indicated for the treatment of *tachycardias*, which are abnormally fast cardiac rhythms. Over 300,000 patients received a new ICD in 2009 alone [27], with 10,000 new patients *every month*. The main task of an ICD is to distinguish between potentially fatal Ventricular Tachycardias (VTs), which originate in the ventricles (lower chambers of the heart) and require an electric shock to terminate them, and usually non-fatal SupraVentricular Tachycardias (SVTs), which originate above the ventricles and can be left to self-terminate. One of the VT/SVT discriminators used in an ICD is a *morphology discriminator (MD)*, which analyzes the morphologies (i.e., shapes) of depolarizations. An MD operates as follows.

- A single *template* depolarization $\mathbf{y}_T$ is recorded by the ICD during normal sinus rhythm (NSR). This represents the normal shape of the depolarization during regular conduction from the atria to the ventricles. See Fig. 1 (b).
- The observed signal is partitioned into single depolarization by what is called a *sensing* algorithm.
- A distance function d takes in the current depolarization $\mathbf{x}$ and the template depolarization $\mathbf{y}_T$ and returns a scalar value $d(\mathbf{x}, \mathbf{y}_T)$ quantifying how different they are.

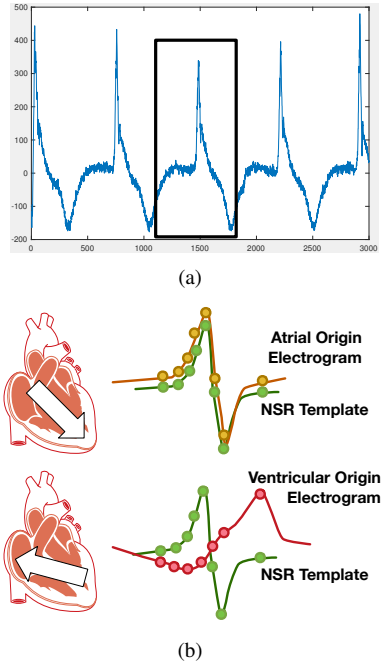

(a)

(b)

Fig. 1. (a) EGM signal with a rectangle around one depolarization. (b) Shapes (a.k.a. *morphologies*) of a single depolarization during an electrical propagation that is supraventricular in origin (top) and ventricular in origin (bottom). The NSR template (green) is a typical depolarization morphology recorded during normal rhythm. The amount of difference between NSR template and current depolarization (red) is used by the ICD to determine the origin of the rhythm.

- If $d(\mathbf{x}, \mathbf{y}_T)$ is less than some pre-set threshold $\alpha \geq 0$, then the two depolarizations are said to match, and the current depolarization is determined to come from a supraventricular rhythm. Otherwise the current depolarization is determined to come from a ventricular rhythm.

We compare the performance of a conformance-based MD to that of two MDs in major-manufacturer ICDs. The first is the Wavelet MD described in [26], [10], and we denote its distance function d_W. The second is Vector Timing and Correlation (VTC) as described in [8], and we denote its distance function d_{VTC}. Due to lack of space, we refer the reader to the references for details.

C. Comparing the discriminators

Because the performance of the three discriminators, and underlying distances, depends on the α thresholds chosen, and these thresholds are programmable in practice and not fixed, we will compare them for a range of thresholds. In what follows the comparison setup is detailed.

A cardiologist has labeled a database of 176 EGM signals from 22 patients, of various durations and displaying different rhythms (NSR, VT, SVT). This number of patients is common in early feasibility studies. The signals were collected in the electrophysiology lab. The patients are all male, with mean age 61 and standard deviation 15 years. For each patient, an NSR template $\mathbf{y}_T$ is acquired from an NSR signal. Each remaining signal is then partitioned into individual depolarizations. The distance $d(\mathbf{x}_k, \mathbf{y}_T)$ between the k^{th} depolarization $\mathbf{x}_k$ and the template $\mathbf{y}_T$ is recorded,

where d is one of ρ_τ, d_W or d_{VTC}. This yields a vector $\Delta = (\delta_1, \ldots, \delta_p)$ of distance values for each patient (The database has a few hundred depolarizations per patient).

For a given distance function, the threshold α can be in a given range $A = [\underline{\alpha}, \overline{\alpha}]$. E.g. the percentage match of WaveletMD is chosen from $[0, 1] \times 100\%$. Therefore, for each distance function and for each value $\alpha \in A$, the distance values in Δ are thresholded. If a given depolarization $\mathbf{x}$ is a true SVT (because it comes from an SVT signal), and $d(\mathbf{x}, \mathbf{y}_T) \leq \alpha$, this is a correct classification. Otherwise, it's an incorrect classification. Analogously, if a given depolarization is a true VT (because it comes from a VT record), it is correctly classified iff $d(\mathbf{x}, \mathbf{y}_T) > \alpha$.

The *sensitivity* and *specificity* of a discriminator at level α are defined as

$$\text{Sensitivity}_\alpha = \frac{\text{Nb. of correctly classified VT depolarizations}}{\text{Total nb of VT depolarizations}}$$

$$\text{Specificity}_\alpha = \frac{\text{Nb. of correctly classified SVT depolarizations}}{\text{Total nb of SVT depolarizations}}$$

By varying α and plotting the points ($\text{Specificity}_\alpha$, $\text{Sensitivity}_\alpha$), we obtain the Sensitivity vs. Specificity curve (SSC). A discriminator performs better if its SSC lies above that of other discriminators: this means that for a given specificity, it achieves a higher sensitivity, and vice-versa.

Choice of τ. The parameter τ needs to be set by the domain experts. Conceivably, it could be optimized over a training set to achieve a desired point on the SSC curve.

III. Results

The results are shown in Fig. 2(a). *We first note that the conformance SSC lies above that of the other two discriminators, clearly indicating it uses a better distance function than those two.* Moreover, the conformance-based MD is minimally affected by the sensing algorithm, which is another sign of its robustness. Next, note that a 100% sensitivity was achieved by the conformance distance function, for all patients, over a wide range of threshold values. This is crucial, since anything less than 100% means that some true, potentially fatal, VT rhythms are missed. Thus in the rest of the results, we may restrict our attention to the threshold values where sensitivity is above 95%.

For each patient, we measured which MDs gave the highest specificity at sensitivity values above 95%. These are the MDs that performed best for this patient. Conformance achieved highest specificity for 13 out of 22 patients, VTC achieved it for 12 patients, and Wavelet for 6 patients. Thus conformance is best for a larger number of patients in this cohort. The first row of Table I summarizes these results.

For those patients where conformance did better, the average relative improvement in specificity over either VTC or WaveletMD was 6.6% (with maximum improvement 18.1%).

Robustness to sensing errors. To study the algorithms' robustness to sensing errors, we re-ran the above experiments, but this time we systematically shifted the individual depolarizations by 5% and 8% of their window length, to model poor partitioning of individual depolarizations, which in turn yields an artificially large distance value. The results are shown in Fig. 2(b). The second and third rows of Table I give the number of patients for which the given distance function produced the highest specificity at a sensitivity above 95%. Here too, conformance does better, especially at higher levels of errors. Moreover, the relative increase in specificity of conformance over VTC is now 232%, and over WaveletMD is 188%. Thus, this study establishes that conformance is a more meaningful measure of distance between EGM signals for the purposes of comparing VT and SVT rhythms.

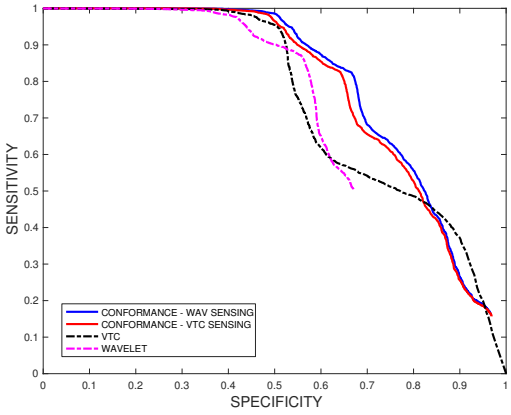

(a) SSC without induced sensing errors.

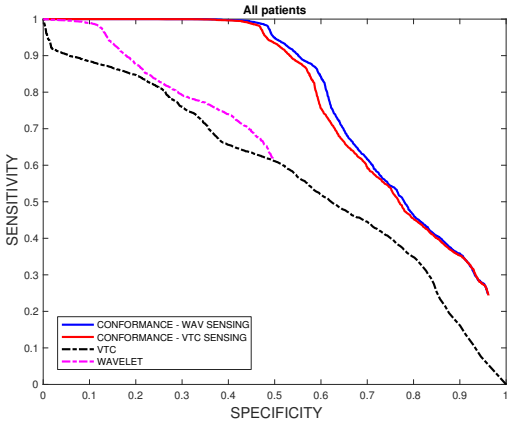

(b) SSC with 8% sensing errors

Fig. 2. Sensitivity vs. Specificity from all patients and signals combined. For conformance-based MD, two curves are shown, corresponding to two different sensing algorithms (ways of partitioning the signal into individual depolarizations). (Colors in on-line version)

TABLE I

Number of patients (out of 22) for which a given distance function achieved the highest specificity. The second and third columns show Conformance-based MDs using different sensing algorithms.

Sensing Error	Conformance WAV Sensing	Conformance VTC Sensing	VTC	WaveletMD
0%	12	13	12	6
5%	15	14	6	5
8%	18	17	3	2

IV. Robust MTL semantics based on conformance

We now turn to the problem of extending robustness-guided falsification (RGF) methods [5], [15] to domains where conformance is the appropriate notion of distance. The main novelty here is that conformance is not a metric: it does not respect the triangle inequality and it does not separate points. All proofs are in the technical report [3].

A. Preliminaries on signal convergence and MTL

We will need a few definitions, which we lift from [18]. Let A be a topological space and $Y \subset A$ a subset of A. Let $\overline{Y}$ denote the closure of Y. Let $f : A \times A \to \mathbb{R}_+$ be a function. Then we define the following derived functions:

$$\begin{aligned} \mathbf{dist}_f(x, Y) &:= \inf_{y \in \overline{Y}} f(x, y) \\ \mathbf{depth}_f(x, Y) &:= \mathbf{dist}_f(x, A \setminus Y) \\ \mathbf{Dist}_f(x, Y) &:= \begin{cases} -\mathbf{dist}_f(x, Y), & x \notin Y \\ \mathbf{depth}_f(x, Y), & x \in Y \end{cases} \end{aligned} \tag{2}$$

For example, if $A = X$ is the state space and $f(x, y) = |x - y|$ is the Euclidian distance between points in X, then the above define, respectively, the distance of a point to a subset $Y \subset X$, the depth of a point in a set, and the signed distance of a point to a set (with positive value indicating the point x is in Y, and a negative value indicating otherwise).

In this paper, we use the notion of *graphical convergence* between signals, since it builds on conformance as the underlying notion of distance between signals, and captures convergence of signals not necessarily supported on the same domain. See [6] for the definition of set convergence.

Definition IV.1 (Graphical convergence [23])**.** *Given a signal $\mathbf{y} \in X^{\mathbb{T}}$, its graph is the set gph$\mathbf{y} := \{(t, y_t) \mid t \in dom\mathbf{y}\}$. A sequence of signals $(\mathbf{y}^i)$ is said to* converge graphically *to a signal $\mathbf{y}$ if the sequence of sets $\{gph\, \mathbf{y}^i\}_i$ converges to the set gph $\mathbf{y}$ in the sense of set convergence. We denote this by $\mathbf{y}^i \xrightarrow{G} \mathbf{y}$.*

1) Metric Temporal Logic and its robust semantics: Metric Temporal Logic (MTL) is a formal language for expressing high-level properties of signals, such as "whenever the signal exceeds the value 500, it eventually goes below 450 within 5 minutes". Formally, let AP be a set of *atomic propositions*. The syntax of MTL formulae is given by

$$\varphi := \ \top \mid p \in AP \mid \neg\varphi \mid \varphi_1 \vee \varphi_2 \mid \varphi_1 \mathcal{U}_I \varphi_2$$

Here, $\neg, \vee, \wedge$ are the boolean connectives Not, Or and And, $\mathcal{U}_I$ is the timed Until operator, and $I \subset \mathbb{T}$ is an interval in $\mathbb{T}$. We write $\bot = \neg\top$, $t + I = \{t + a \mid a \in I\}$. In all that follows, we will assume, without loss of generality, that AP contains p iff it contains its negation $\neg p$.

Let $\mathcal{O} : AP \to \mathcal{P}(X)$ be a function that maps atomic propositions to the subsets of the state space that satisfy them. The *boolean semantics* of MTL formulae map a formula to $\{\top, \bot\}$ as follows.

Definition IV.2 (Boolean semantics)**.**

$$\begin{aligned} \forall p \in AP,\ \ll p, \mathcal{O} \gg (\mathbf{x}, t) &\Leftrightarrow x_t \in \mathcal{O}(p) \\ \ll \neg\varphi, \mathcal{O} \gg (\mathbf{x}, t) &\Leftrightarrow \neg \ll \varphi, \mathcal{O} \gg \\ \ll \varphi_1 \vee \varphi_2, \mathcal{O} \gg (\mathbf{x}, t) &\Leftrightarrow \ll \varphi_1, \mathcal{O} \gg \vee \ll \varphi_2, \mathcal{O} \gg \\ \ll \varphi_1 \mathcal{U}_I \varphi_2, \mathcal{O} \gg (\mathbf{x}, t) &\Leftrightarrow \exists t' \in t + I \cap \mathbb{T}\ .\ \ll \varphi_2, \mathcal{O} \gg (\mathbf{x}, t') \\ &\quad \wedge \forall t'' \in [t, t')\ \ll \varphi_1, \mathcal{O} \gg (\mathbf{x}, t'') \end{aligned}$$

If $\ll \varphi, \mathcal{O} \gg (\mathbf{x}, t) = \top$, we write $(\mathbf{x}, t) \models \varphi$. Informally, $\varphi_1 \mathcal{U}_I \varphi_2$ says that at some point in $t + I$, φ_2 holds, and at every moment between now (t) and then, φ_1 holds. The other connectives have their usual boolean meaning.

The **robust semantics** of MTL how *robustly* $\mathbf{x}$ satisfies (or falsifies) φ. Let $\rho : X^{\mathbb{T}} \times X^{\mathbb{T}} \to \mathbb{R}_+$ be the sup metric, $\rho(\mathbf{x}, \mathbf{y}) = \sup_{t \in \mathbb{T}} |x_t - y_t|$. Let $\mathcal{L}_t(\varphi) \subset X^{\mathbb{T}}$ be the set of signals that satisfy φ starting at time $t \in \mathbb{T}$, that is, $\mathcal{L}_t(\varphi) = \{\mathbf{x} \in X^{\mathbb{T}} \mid (\mathbf{x}, t) \models \varphi\}$.

Definition IV.3 ((Spatial) Robustness degree [19])**.** *The* robustness degree *of the MTL formula φ relative to $\mathbf{x}$ starting at t is defined as $\mathbf{Dist}_\rho(\mathbf{x}, \mathcal{L}_t(\varphi))$.*

Thus the robustness degree provides a precise sense for how much disturbance a signal can tolerate while still satisfying (or falsifying) the specification:

Theorem IV.1 ([19])**.** *Let $\mathbf{x} \in X^{\mathbb{T}}$. For every $\mathbf{y} \in X^{\mathbb{T}}$ s.t. $\rho(\mathbf{x}, \mathbf{y}) < \mathbf{Dist}_\rho(\mathbf{x}, \mathcal{L}_t(\varphi))$, it holds that $\ll \varphi, \mathcal{O} \gg (\mathbf{x}, t) = \ll \varphi, \mathcal{O} \gg (\mathbf{y}, t)$.*

The robustness degree cannot be directly computed because $\mathcal{L}_t(\varphi)$ cannot be conveniently characterized. The *robust semantics* of MTL formulae provide a way to approximate the robustness degree by performing simple computations on the signal $\mathbf{x}$ itself. Let $d : X \times X \to \mathbb{R}_+$ be a metric defined on X.

Definition IV.4 ((Spatial) Robust semantics)**.**

$$\begin{aligned} [\![\top, \mathcal{O}]\!](\mathbf{x}, t) &= +\infty \\ \forall p \in AP,\ [\![p, \mathcal{O}]\!](\mathbf{x}, t) &= \mathbf{Dist}_d(x_t, \mathcal{O}(p)) \\ [\![\neg\varphi, \mathcal{O}]\!](\mathbf{x}, t) &= -[\![\varphi, \mathcal{O}]\!](\mathbf{x}, t) \\ [\![\varphi_1 \vee \varphi_2, \mathcal{O}]\!](\mathbf{x}, t) &= [\![\varphi_1, \mathcal{O}]\!](\mathbf{x}, t) \vee [\![\varphi_2, \mathcal{O}]\!](\mathbf{x}, t) \\ [\![\varphi_1 \wedge \varphi_2, \mathcal{O}]\!](\mathbf{x}, t) &= [\![\varphi_1, \mathcal{O}]\!](\mathbf{x}, t) \wedge [\![\varphi_2, \mathcal{O}]\!](\mathbf{x}, t) \\ [\![\varphi_1 \mathcal{U}_I \varphi_2, \mathcal{O}]\!](\mathbf{x}, t) &= \sqcup_{t' \in t +_{\mathbb{T}} I} \Big([\![\varphi_2, \mathcal{O}]\!](\mathbf{x}, t') \sqcap \\ &\quad \sqcap_{t'' \in [t, t')} [\![\varphi_1, \mathcal{O}]\!](\mathbf{x}, t'') \Big) \end{aligned}$$

The main property of the robust semantics, which justifies its usefulness, is captured in the following theorem:

Theorem IV.2 ([19])**.** *For any MTL formula φ, signal $\mathbf{x} \in X^{\mathbb{T}}$, time $t \in \mathbb{T}$ and map $\mathcal{O}$, it holds that*

$$-\mathbf{dist}_\rho(\mathbf{x}, \mathcal{L}_t(\varphi)) \leq [\![\varphi, \mathcal{O}]\!](\mathbf{x}, t) \leq \mathbf{depth}_\rho(\mathbf{x}, \mathcal{L}_t(\varphi))$$

Thus if $[\![\varphi, \mathcal{O}]\!](\mathbf{x}, t) > 0$, then $\mathbf{depth}_\rho(\mathbf{x}, \mathcal{L}_t(\varphi)) > 0$ and $(\mathbf{x}, t) \models \varphi$. On the other hand, if $[\![\varphi, \mathcal{O}]\!](\mathbf{x}, t) < 0$, then $(\mathbf{x}, t) \not\models \varphi$. Putting the two sides of the inequality together it holds that

$$|[\![\varphi, \mathcal{O}]\!](\mathbf{x}, t)| \leq |\mathbf{Dist}_\rho(\mathbf{x}, \mathcal{L}_t(\varphi))| \tag{3}$$

Robustness-Guided Falsification [20] searches for system executions $\mathbf{x}$ that falsify φ by minimizing $[\![\varphi, \mathcal{O}]\!](\mathbf{x}, t)$ over the (deterministic) system's initial conditions. If a negative robustness is found, then the trace with the negative robustness witnesses a falsification.

B. Robust MTL semantics using conformance

We now show that if we substitute our conformance distance ρ_τ for the metric ρ in defining the robust semantics, then the conclusions of Thms. IV.1 and IV.2 still hold.

Definition IV.5. *Fix $\tau > 0$. Let S be a subset of X, $\mathbf{x} \in X^{\mathbb{T}}$ be a signal defined on $\mathbb{T}$, and let $t \in \mathbb{T}$. The point-to-set distance is given by*

$$psd_\tau(\mathbf{x}, t, S) := \inf_{y \in \overline{S}} \inf_{s : |s-t| \leq \tau} |x_s - y| \tag{4}$$

Two things are noteworthy about the distances in (1) and (4). First, is that d_τ is only defined for points in X that are on some trajectories $\mathbf{x}$ and $\mathbf{y}$. It is not defined everywhere on X. Secondly, the point-to-set distance psd is *not* defined using d_τ: indeed the set S is an arbitrary subset of X.

We define the conformance-based robustness degree to be $\mathbf{Dist}_{\rho_\tau}(\mathbf{x}, \mathcal{L}_t(\varphi))$ (recall the definitions in (2)). The next result shows that the conclusion of Thm. IV.1 still holds. The proof is immediate and we skip it.

Theorem IV.3. *Let $\mathbf{x} \in X^{\mathbb{T}}$. For any signal $\mathbf{y} \in X^{\mathbb{T}}$ s.t. $\rho_\tau(\mathbf{x}, \mathbf{y}) < \mathbf{Dist}_{\rho_\tau}(\mathbf{x}, \mathcal{L}_t(\varphi))$, it holds that $\ll \varphi, \mathcal{O} \gg (\mathbf{x}, t) = \ll \varphi, \mathcal{O} \gg (\mathbf{y}, t)$.*

As before, $\mathbf{Dist}_{\rho_\tau}(\mathbf{x}, \mathcal{L}_t(\varphi))$ cannot be computed. Therefore we define the robust semantics as before, only now using the weaker notion of dissimilarity ρ_τ between signals.

Definition IV.6 (Conformance robust semantics)**.**

$$\begin{aligned}
[\![\top, \mathcal{O}]\!]_{\rho_\tau}(\mathbf{x}, t) &= +\infty \\
\forall p \in AP,\ [\![p, \mathcal{O}]\!]_{\rho_\tau}(\mathbf{x}, t) &= \begin{cases} psd_\tau(\mathbf{x}, t, X \setminus \mathcal{O}(p)), & \text{if } x \in \mathcal{O}(p) \\ -psd_\tau(\mathbf{x}, t, \mathcal{O}(p)), & \text{if } x \notin \mathcal{O}(p) \end{cases} \\
[\![\neg\varphi, \mathcal{O}]\!]_{\rho_\tau}(\mathbf{x}, t) &= -[\![\varphi, \mathcal{O}]\!]_{\rho_\tau}(\mathbf{x}, t) \\
[\![\varphi_1 \vee \varphi_2, \mathcal{O}]\!]_{\rho_\tau}(\mathbf{x}, t) &= [\![\varphi_1, \mathcal{O}]\!]_{\rho_\tau}(\mathbf{x}, t) \sqcup [\![\varphi_2, \mathcal{O}]\!]_{\rho_\tau}(\mathbf{x}, t) \\
[\![\varphi_1 \mathcal{U}_I \varphi_2, \mathcal{O}]\!]_{\rho_\tau}(\mathbf{x}, t) &= \sqcup_{t' \in t +_{\mathbb{T}} I} \Big([\![\varphi_2, \mathcal{O}]\!]_{\rho_\tau}(\mathbf{x}, t') \\
&\qquad \bigsqcap \sqcap_{t'' \in [t, t')} [\![\varphi_1, \mathcal{O}]\!]_{\rho_\tau}(\mathbf{x}, t'') \Big)
\end{aligned}$$

The next result shows that the robust semantics founded on conformance maintain the desirable property of approximating the robustness degree founded on conformance. It allows us to use the machinery of RGF to search over a heart model's parameters to find fatal arrhythmic behavior, by minimizing the robustness of the output EGM signals relative to a specification describing the arrhythmia of interest.

Theorem IV.4. *For any MTL formula φ, signal $\mathbf{x} \in X^{\mathbb{T}}$, time $t \in \mathbb{T}$ and map $\mathcal{O}$, it holds that*

$$-\mathbf{dist}_{\rho_\tau}(\mathbf{x}, \mathcal{L}_t(\varphi)) \leq [\![\varphi, \mathcal{O}]\!]_{\rho_\tau}(\mathbf{x}, t) \leq \mathbf{depth}_{\rho_\tau}(\mathbf{x}, \mathcal{L}_t(\varphi)) \tag{5}$$

This theorem also allows us to use the same efficient dynamic programming algorithm used in [14] to monitor the new semantics. The following theorem relates conformance-based and sup norm-based robust semantics from Def. IV.4.

Theorem IV.5. *1. For any signal $\mathbf{x}$ and formula φ, the following inequality holds, and it is tight.*

$$|[\![\varphi, \mathcal{O}]\!]_{\rho_\tau}(\mathbf{x}, t)| \leq |[\![\varphi, \mathcal{O}]\!](\mathbf{x}, t)|$$

2. Let S be a subset of signals sharing the same domain $\mathbb{T}$ and which are continuous on $\mathbb{T}$. Then as $\tau \to 0$, $\rho_\tau \to \rho$ on S and $[\![\varphi, \mathcal{O}]\!]_{\rho_\tau}(\mathbf{x}, t) \to [\![\varphi, \mathcal{O}]\!](\mathbf{x}, t)$ for any $\mathbf{x} \in S$.

C. Conformance-based temporal robustness

In [16] another robust semantics was introduced, which quantifies how much to shift the signal *in time* in order to change its truth value relative to a specification φ. Let $[\![\cdot, \cdot]\!]_\chi$ denote the sup norm-based temporal semantics introduced in [16]. We may also define a *temporal* conformance distance by a natural adaptation of the above definitions. The resulting robust semantics generalize the usual $[\![\cdot, \cdot]\!]_\chi$, much in the same way that $[\![\varphi, \mathcal{O}]\!]_{\rho_\tau}$ generalizes $[\![\varphi, \mathcal{O}]\!]$ (Thm. IV.5).

Specifically, given $\varepsilon > 0$, for every 2 signals $\mathbf{x}, \mathbf{y} \in X^{\mathbb{T}}$ define the time shift function $\overrightarrow{u}_\varepsilon(\mathbf{x}, \mathbf{y}, t) = \inf\{\tau > 0 \mid \inf_{s : |s-t| < \tau} |x_t - y_s| < \varepsilon\}$, and $\chi_\varepsilon(\mathbf{x}, \mathbf{y}) = \sup_{t \in \mathbb{T}}(\overrightarrow{u}_\varepsilon(\mathbf{x}, \mathbf{y}, t) \sqcup \overrightarrow{u}_\varepsilon(\mathbf{y}, \mathbf{x}, t))$. Given a set $S \subset X$, define $psdt_\varepsilon(\mathbf{x}, t, S) = \inf\{\tau > 0 \mid \inf_{s : |s-t| < \tau, y \in \overline{S}} |x_s - y| < \varepsilon\}$. We can now define temporal robustness, $[\![\cdot, \cdot]\!]_{\chi_\varepsilon}$ using Def. IV.6 but using $psdt_\varepsilon$ instead of psd_τ. The following is the temporal equivalent of Thm. IV.5, with a similar proof using χ_ε instead of d_τ.

Theorem IV.6. *For every $\varepsilon > 0$, formula φ, signal $\mathbf{x} \in X^{\mathbb{T}}$ and $t \in \mathbb{T}$, $[\![\varphi, \mathcal{O}]\!]_{\chi_\varepsilon} \leq [\![\varphi, \mathcal{O}]\!]_\chi$*

V. Illustrative Examples

Keeping within the focus of this paper, we will now illustrate Thm. IV.5. The characterization of an SVT signal is complex, and patient-specific. The following two formulas offer a partial characterization. Let $\theta > 0$ and $a < b < c < d < e < f$, $g < g' < h$. The operator $\Box$ is 'Always' and $\Diamond$ means 'Eventually'. Both are derived from $\mathcal{U}$.

$$\begin{aligned}
\varphi_{rate} = \Box_{[0,T]}\big((\Box_{[a,b]} x > \theta) \implies \big(\Diamond_{[b,c]} x \leq \theta\big) \\
\wedge \big(\Diamond_{[d,e]}(\Box_{[0,f]} x > \theta)\big)\big)
\end{aligned}$$

$$\varphi_{width} = \Box_{[0,T]}\big((x < \theta \wedge \Diamond_{[g,g']} x > \theta) \implies \Box_{[g',h]} x > \theta\big)$$

φ_{rate} establishes bounds on the rhythm's rate, which is one of the most important features of a heart rhythm.[2] φ_{width} places a minimum on the width of the main deflection of the signal, which is an indirect measurement of signal propagation speed in the heart. We measured the conformance-based semantics and usual sup norm-based semantics of these two formulas with respect to a cardiac signal $\mathbf{x}$ with quasi-period 800ms. For $\tau = 5$ms, the results were

$$[\![\varphi_{width}, \mathcal{O}]\!]_{\rho_\tau}(\mathbf{x}, 0) = 0.6621 < [\![\varphi_{width}, \mathcal{O}]\!](\mathbf{x}, 0) = 1.2441$$

[2]From a theoretical perspective, rate might be better tackled in the frequency domain. But cardiac implantable devices avoid or greatly simplify frequency transformations to reduce energy consumption and delays.

$$[\![\varphi_{rate}, \mathcal{O}]\!]_{\rho_\tau}(\mathbf{x}, 0) = 0.4377 < [\![\varphi_{rate}, \mathcal{O}]\!](\mathbf{x}, 0) = 1.6814$$

Even though 5ms is a small window relative to the signal quasi-period of 800ms, the difference between the appropriate, conformance-based semantics, and the sup norm-based semantics, is significant. If the latter are used in robustness-guided falsification, then a large minimum robustness might be concealing what is actually non-robust behavior. This highlights the necessity of using the appropriate distance and associated semantics.

If $\tau = 0$ (which we can do in experiments since the signals are sampled at the same rate), the robustness values $[\![\varphi, \mathcal{O}]\!]_{\rho_\tau}$ and $[\![\varphi, \mathcal{O}]\!]_{\rho}$ are equal as predicted.

VI. Related work

Conformance was introduced in [4], based on [23], as a distance between the executions of hybrid systems, that relaxes both temporal and spatial matching constraints. A number of closeness measures between hybrid trajectories and systems exist. Measures based on bisimulation [21] and supnorms [9] only consider the differences in signal values at the same moment in time. Other closeness measures, conversely, consider only differences in trajectories' timing, e.g., [24]. The Skorokhod metric used in [11], [13] and generalized in [12] measures the norm of the *retiming* needed to make two signals match, and it is not clear how this can be leveraged to define a point-to-set distance in our context. See [7] for issues relating to learning domain-appropriate pseudo-metrics. The weighted edit distance was used to define quantitative semantics for STL in [25] but it only applies to finite-length, finite-range signals, which are unnecessary restrictions is necessary in our setup.

VII. Conclusion

The application of systems methods to the medical and biological fields must take into account the specific character of the new types of signals in these fields. In cardiac electrophysiology, electrograms are complex, noisy, non-parametric and highly variable across patients and within a patient over time. We have shown that in the task of arrhythmia discrimination, conformance is the suitable distance over electrogram space. Despite it not being nearly as well-behaved as a metric, we showed that robustness-guided falsification can still be applied in a principled manner, and that using the usual sup norm-based robustness yields false and misleading results. Moving forward, we will develop a heart model that allows us to search its parameter space for arrhythmias and test it in-the-loop with a defibrillator.

References

[1] H. Abbas, K. J. Jang, J. Liang, S. Dixit, and R. Mangharam. A novel morphology discriminator to improve discrimination between ventricular and supraventricular tachycardias. *Heart Rhythm Journal (Supplement)*, 14(5), May 2017.

[2] H. Abbas, K. J. Jiang, Z. Jiang, and R. Mangharam. Towards model checking of implantable cardioverter defibrillators. In *Proceedings of the 19th International Conference on Hybrid Systems: Computation and Control*, HSCC '16, pages 87–92, New York, NY, USA, 2016. ACM.

[3] H. Abbas and R. Mangharam. Technical report: Generalized robust MTL semantics for problems in cardiac electrophysiology. Online at http://www.seas.upenn.edu/∼habbas/publications/papers/ACC18.pdf, January 2018.

[4] H. Abbas, H. Mittelmann, and G. Fainekos. Formal property verification in a conformance testing framework. In *MEMOCODE*, 2014.

[5] Y. S. R. Annapureddy and G. E. Fainekos. Ant colonies for temporal logic falsification of hybrid systems. In *Proc. of the 36th Annual Conference of IEEE Industrial Electronics*, pages 91–96, 2010.

[6] J. P. Aubin. *Viability Theory*. Birkhauser, 1991.

[7] A. Bellet, A. Harbard, and M. Sebban. A survey on metric learning for feature vectors and structured data. *Arxiv*, 2014.

[8] Boston Scientific Corporation. The Compass - Technical Guide to Boston Scientific Cardiac Rhythm Management Products. *Device Documentation*, 2007.

[9] S. Burden, H. Gonzales, R. Vasudevan, R. Bajcsy, and S. S. Sastry. Metrization and simulation of controlled hybrid systems. Technical Report arXiv:1302.4402, February 2013.

[10] C. D. Swerdlow et al . Discrimination of Ventricular Tachycardia from Supraventricular Tachycardia by a Downloaded Wavelet Transform Morphology Algorithm: A Paradigm for Development of Implantable Cardioverter Defibrillator Detection Algorithms. *J. Cardiovascular Electrophysiology*, 13, 2002.

[11] P. Caspi and A. Benveniste. Toward an approximation theory for computerized control. In *Embedded Software*, volume 2491 of *LNCS*, pages 294–304. Springer, 2002.

[12] J. Davoren. Epsilon-tubes and generalized skorokhod metrics for hybrid paths spaces. In R. Majumdar and P. Tabuada, editors, *Hybrid Systems: Computation and Control*, volume 5469 of *LNCS*, pages 135–149. Springer, 2009.

[13] J. V. Deshmukh, R. Majumdar, and V. S. Prabhu. Quantifying conformance using the skorokhod metric. *Formal Methods in System Design*, 50(2):168–206, Jun 2017.

[14] A. Dokhanchi, B. Hoxha, and G. Fainekos. On-line monitoring for temporal logic robustness. In *Runtime Verification*. Springer, 2014.

[15] A. Donzé. Breach, a toolbox for verification and parameter synthesis of hybrid systems. In *Proceedings of the 22Nd International Conference on Computer Aided Verification*, CAV'10, pages 167–170, Berlin, Heidelberg, 2010. Springer-Verlag.

[16] A. Donzé and O. Maler. *Robust Satisfaction of Temporal Logic over Real-Valued Signals*, pages 92–106. Springer Berlin Heidelberg, Berlin, Heidelberg, 2010.

[17] K. Ellenbogen, G. N. Kay, C.-P. Lau, and B. L. Wilkoff. *Clinical Cardiac Pacing, Defibrillation, and Resynchronization Therapy*. Elsevier, 2011.

[18] G. Fainekos. *Robustness of Temporal Logic Specifications*. PhD thesis, University of Pennsylvania, 2008.

[19] G. Fainekos and G. Pappas. Robustness of temporal logic specifications for continuous-time signals. *Theoretical Computer Science*, 410(42):4262–4291, September 2009.

[20] G. Fainekos, S. Sankaranarayanan, K. Ueda, and H. Yazarel. Verification of automotive control applications using s-taliro. In *Proceedings of the American Control Conference*, 2012.

[21] A. Girard, A. Julius, and G. Pappas. Approximate simulation relations for hybrid systems. *Discrete Event Dynamic Systems*, 18(2):163–179, 2008.

[22] R. Goebel, R. G. SanFelice, and A. R. Teel. *Hybrid Dynamical Systems: modeling, stability and robustness*. Princeton University Press, 2012.

[23] R. Goebel and A. Teel. Solutions to hybrid inclusions via set and graphical convergence with stability theory applications. *Automatica*, 42(4):573 – 587, 2006.

[24] J. Huang, J. Voeten, and M. Geilen. Real-time property preservation in approximations of timed systems. In *Formal Methods and Models for Co-Design, 2003. MEMOCODE '03. Proceedings. First ACM and IEEE International Conference on*, pages 163–171, June 2003.

[25] S. Jakšić, E. Bartocci, R. Grosu, and D. Ničković. *Quantitative Monitoring of STL with Edit Distance*, pages 201–218. Springer International Publishing, Cham, 2016.

[26] L. Koyrakh, J. Gillberg, and N. Wood. Wavelet transform based algorithms for EGM morphology discrimination for implantable ICDs. In *Computers in Cardiology, 1999*, pages 343–346, 1999.

[27] H. G. Mond and A. Proclemer. The 11th world survey of cardiac pacing and implantable cardioverter-defibrillators: Calendar year 2009.

a world society of arrhythmia's project. *Pacing and Clinical Electrophysiology*, 34(8):1013–1027, 2011.

APPENDIX

PROOF OF THM. IV.4

For the proof we will need the following lemma.

Lemma .1. *Given signals* $\mathbf{x}$ *and* $\mathbf{y}$*, and a set of signals* S*. Let* $\overline{S}$ *be the closure of* S*, that is,* $\overline{S} = S \cup \partial S$ *where* $\partial S = \{\mathbf{z} \in X^{\mathbb{T}} \mid \exists (\mathbf{z}_i) : \mathbf{z}_i \overset{G}{\to} \mathbf{z}\}$*. Then* $\inf_{\mathbf{y}\in S} \rho_\tau(\mathbf{x},\mathbf{y}) = \inf_{\mathbf{y}\in\overline{S}} \rho_\tau(\mathbf{x},\mathbf{y})$.

Proof. Write $r = \rho_\tau(\mathbf{x},\mathbf{y})$. We establish that $\inf_{\mathbf{y}\in S} \rho_\tau(\mathbf{x},\mathbf{y}) \leq \inf_{\mathbf{y}\in\overline{S}} \rho_\tau(\mathbf{x},\mathbf{y})$, the other direction being immediate. Now let $(\mathbf{y}^i) \in S$ be a sequence of signals that converges graphically to $\mathbf{y}$. Since $\inf_{\mathbf{y}\in S} \rho_\tau(\mathbf{x},\mathbf{y}) \leq \liminf_{i\to\infty} \rho_\tau(\mathbf{x},\mathbf{y}^i)$[3], it suffices to show that

$$\liminf_{i\to\infty} \rho_\tau(\mathbf{x},\mathbf{y}^i) \leq \rho_\tau(\mathbf{x},\mathbf{y}) \tag{6}$$

This yields the desired inequality by taking the inf on both sides.

Assume (6) to not hold for a contradiction. Then there exists an $i_0 \in \mathbb{N}$ and a $\delta > 0$ s.t. $\rho_\tau(\mathbf{x},\mathbf{y}^i) \geq r + \delta$ for all $i > i_0$. For every x_t, there exists $y_{s(t)}$ s.t. $|t - s(t)| < \tau$ and $|x_t - y_{s(t)}| \leq r$. Define $a = \inf_{t\in\mathbb{T}} \min(|s(t) - (t - \tau)|, |s(t) - (t + \tau)|)$: this is the closest that the matching time $s(t)$ gets to the ends of the interval $[t-\tau, t+\tau]$. Since the domains of our signals are bounded and $|s(t) - t| < \tau$, it holds that $a > 0$. Similarly, for every $s \in \operatorname{dom}\mathbf{y}$ there exists a $t(s) \in \operatorname{dom}\mathbf{x}$ s.t. $|s - t(s)| < \tau$ and $|x_{t(s)} - y_s| \leq r$. Define $b = \inf_{t\in\mathbb{T}} \min(|t(s) - (s - \tau)|, |t(s) - (s + \tau)|)$: this is the closest that the matching time $t(s)$ gets to the ends of the interval $[s-\tau, s+\tau]$. It also holds that $b > 0$. Let $\omega = \min(\delta/2, \tau, a/2, b/2) > 0$. Now recall that $\mathbf{y}_i$ converges to $\mathbf{y}$ graphically, so by [22, Thm. 5.25] there exists an integer $i_1 > i_0$ s.t. for all $i > i_1$, the following holds: for every $y_{s(t)}$ there exists $y^i_{s'}$ s.t. $|s(t) - s'| < \omega$ and $|y_{s(t)} - y^i_{s'}| < \omega$. This implies that for all $i > i_1$

$$\begin{aligned} &|t - s'| \leq |t - s(t)| + |s(t) - s'| \leq \tau - a + a/2 < \tau \\ &\text{and } |x_t - y^i_{s'}| \leq |x_t - y_{s(t)}| + |y_{s(t)} - y^i_{s'}| < r + \delta/2 \end{aligned} \tag{7}$$

Conversely, [22, Thm. 5.25] also implies that for every $s' \in \operatorname{dom}\mathbf{y}^i$, there exists $s \in \operatorname{dom}\mathbf{y}$ s.t. $|s - s'| < \omega$ and $|y_s - y^i_{s'}| < \omega$. There also exists $t \in \operatorname{dom}\mathbf{x}$ s.t. $|t - s| < \tau$ and $|\mathbf{x}_t - \mathbf{y}_s| \leq r$. This implies that

$$|t - s'| \leq \tau - b + b/2 < \tau \text{ and } |x_t - y^i_{s'}| < r + \delta/2 \tag{8}$$

Putting (7) and (8) together yields $\rho_\tau(\mathbf{x},\mathbf{y}^i) < r + \delta/2$ for every $i > i_1$, a contradiction. This concludes the proof. □

We now proceed with the proof of Thm. IV.4. We give the proof for the base cases. The other cases follow by structural induction on φ along the lines of the proofs in [19] with some simple modifications. Recall our assumption that $p \in AP$ iff $\neg p \in AP$, without loss of generality.

Case 1: $\varphi = \top$. Then $\mathcal{L}_t(\varphi) = X^{\mathbb{T}}$ for any t so $\mathbf{depth}_{\rho_\tau}(\mathbf{x}, \mathcal{L}_t(\varphi)) = \mathbf{dist}_{\rho_\tau}(\mathbf{x}, \emptyset) = \infty$ by convention. Also, $-\mathbf{dist}_{\rho_\tau}(\mathbf{x}, X^{\mathbb{T}}) = 0$ so this case holds.

Case 2: $\varphi = p \in AP$.

Case 1.1: $\mathbf{x} \in \mathcal{L}_t(p)$. $\mathbf{Dist}_{\rho_\tau}(\mathbf{x}, \mathcal{L}_t(p)) = \mathbf{depth}_{\rho_\tau}(\mathbf{x}, \mathcal{L}_t(p)) = \mathbf{dist}_{\rho_\tau}(\mathbf{x}, X^{\mathbb{T}} \setminus \mathcal{L}_t(p)) = \inf_{\mathbf{y}\in\overline{X^{\mathbb{T}}\setminus\mathcal{L}_t(p)}} \rho_\tau(\mathbf{x},\mathbf{y}) = \inf_{\mathbf{y}\in X^{\mathbb{T}}\setminus\mathcal{L}_t(p)} \rho_\tau(\mathbf{x},\mathbf{y})$ (by Lemma .1) $= \inf_{\mathbf{y}\in\mathcal{L}_t(\neg p)} \rho_\tau(\mathbf{x},\mathbf{y}) = \inf_{\mathbf{y}\in\mathcal{L}_t(\neg p)} \left[\sup_{t'\neq t} d_\tau(x_{t'}, y_{t'}) \sqcup d_\tau(x_t, y_t)\right]$.

Intuitively, only the value of $\mathbf{y}$ around t should matter. Indeed, for any $\mathbf{z} \in \mathcal{L}_t(\neg p)$ s.t.

$$\sup_{t'\neq t} d_\tau(x_{t'}, z_{t'}) > d_\tau(x_t, z_t) \tag{9}$$

we can build a $\mathbf{z}' \in \mathcal{L}_t(\neg p)$ s.t. $\mathbf{z}'(t') = \mathbf{x}(t')$ for all $t' \neq t$ and $\mathbf{z}'(t) = \mathbf{z}(t)$. Then $\rho_\tau(\mathbf{x},\mathbf{z}') = d_\tau(\mathbf{x},\mathbf{z},t) < \sup_{t'\neq t} d_\tau(\mathbf{x},\mathbf{z},t') \leq \rho_\tau(\mathbf{x},\mathbf{z})$. So we may restrict our attention to signals $\mathbf{y} \in \mathcal{L}_t(\neg p)$ for which (9) does not hold. So $\mathbf{depth}_{\rho_\tau}(\mathbf{x}, \mathcal{L}_t(p))$ equals

$$\begin{aligned} &\inf_{\mathbf{y}\in\mathcal{L}_t(\neg p)} \left[\sup_{t'\neq t} d_\tau(\mathbf{x},\mathbf{y},t') \sqcup d_\tau(\mathbf{x},\mathbf{y},t)\right] \\ = &\inf_{\mathbf{y}\in\mathcal{L}_t(\neg p)} d_\tau(\mathbf{x},\mathbf{y},t) \\ \geq &\inf_{\mathbf{y}\in\mathcal{L}_t(\neg p)} \overrightarrow{d}_\tau(\mathbf{x},\mathbf{y},t) \sqcup \inf_{\mathbf{y}\in\mathcal{L}_t(\neg p)} \overrightarrow{d}_\tau(\mathbf{x},\mathbf{y},t) \end{aligned}$$

Now note that as $\mathbf{y}$ spans $\mathcal{L}_t(\neg p)$, $y_{s\neq t}$ spans all of Xso for any $s \in \mathbb{T}$ s.t. $|s - t| \leq \tau$, there exists $\tilde{\mathbf{y}} \in \mathcal{L}_t(\neg p)$ s.t. $\tilde{y}_s = x_t$, and it follows that

$$\inf_{\mathbf{y}\in\mathcal{L}_t(\neg p)} \overrightarrow{d}_\tau(\mathbf{x},\mathbf{y},t) = \inf_{\mathbf{y}\in\mathcal{L}_t(\neg p)} \inf_{s:|s-t|\leq\tau} |x_t - y_s| = 0$$

On the other hand, as $\mathbf{y}$ spans $\mathcal{L}_t(\neg p)$, y_t spans all of $X \setminus \mathcal{O}(p)$. Therefore

$$\begin{aligned} &\inf_{\mathbf{y}\in\mathcal{L}_t(\neg p)} \overrightarrow{d}_\tau(\mathbf{y},\mathbf{x},t) \\ &\qquad = \inf_{\mathbf{y}\in\mathcal{L}_t(\neg p)} \inf_{s:|s-t|\leq\tau} |y_t - x_s| \\ &\qquad = \inf_{\bar{y}\in X\setminus\mathcal{O}(p)} \inf_{s:|s-t|\leq\tau} |x_s - \bar{y}| \\ &\qquad = psd_\tau(\mathbf{x}, t, X \setminus \mathcal{O}(p)) \\ &\qquad = [\![p, \mathcal{O}]\!]_{\rho_\tau}(\mathbf{x}, t) \geq 0 \end{aligned}$$

It comes that $\mathbf{depth}_{\rho_\tau}(\mathbf{x}, \mathcal{L}_t(p)) \geq 0 \sqcup [\![p, \mathcal{O}]\!]_{\rho_\tau}(\mathbf{x}, t) = [\![p, \mathcal{O}]\!]_{\rho_\tau}(\mathbf{x}, t)$.

For the other side of the inequality, we note that $\mathbf{dist}_{\rho_\tau}(\mathbf{x}, \mathcal{L}_t(p)) = \inf_{\mathbf{y}\in\mathcal{L}_t(p)} \rho_\tau(\mathbf{x},\mathbf{y}) = 0$ since $\mathbf{x} \in \mathcal{L}_t(p)$.

Case 1.2: $\mathbf{x} \notin \mathcal{L}_t(p)$. Define $p' = \neg p \in AP$. Then by previous case, $0 \leq [\![p', \mathcal{O}]\!]_{\rho_\tau}(\mathbf{x}, t) \leq \mathbf{depth}_{\rho_\tau}(\mathbf{x}, \mathcal{L}_t(p'))$, which is equivalent to

$$-\mathbf{depth}_{\rho_\tau}(\mathbf{x}, \mathcal{L}_t(p)) \leq -[\![p', \mathcal{O}]\!]_{\rho_\tau}(\mathbf{x}, t) = [\![p, \mathcal{O}]\!]_{\rho_\tau}(\mathbf{x}, t) \leq 0$$

[3] We haven't shown continuity of ρ_τ so even though $\mathbf{y}^i$ converges to $\mathbf{y}$, ρ_τ may have several accumulation points at the convergence point $\mathbf{y}$, whence the use of $\liminf$. The inequality can be readily shown by contradiction: assume $a := \liminf f(x_i) < f_* := \inf_{x\in S} f(x)$ and use the definition of accumulation point: $\forall\varepsilon > 0, \forall i_0, \exists i > i_0 \,.\, |f(x_i) - a| < \varepsilon$.

Now $\mathbf{depth}_{\rho_\tau}(\mathbf{x}, \mathcal{L}_t(p)) = 0$ and $\mathbf{depth}_{\rho_\tau}(\mathbf{x}, \mathcal{L}_t(p')) = \mathbf{dist}_{\rho_\tau}(\mathbf{x}, \mathcal{L}_t(p))$. This concludes this case.

Case 2: $\varphi = \neg\varphi_1$. By the induction hypothesis,

$$-\mathbf{dist}_{\rho_\tau}(\mathbf{x}, \mathcal{L}_t(\varphi_1)) \leq [\![\varphi_1, \mathcal{O}]\!]_{\rho_\tau}(\mathbf{x}, t) \leq \mathbf{depth}_{\rho_\tau}(\mathbf{x}, \mathcal{L}_t(\varphi_1))$$
$$-\mathbf{depth}_{\rho_\tau}(\mathbf{x}, \mathcal{L}_t(\varphi_1)) \leq [\![\varphi_1, \mathcal{O}]\!]_{\rho_\tau}(\mathbf{x}, t) \leq \mathbf{dist}_{\rho_\tau}(\mathbf{x}, \mathcal{L}_t(\varphi_1))$$

Now $-\mathbf{depth}_{\rho_\tau}(\mathbf{x}, \mathcal{L}_t(\varphi_1)) = -\mathbf{dist}_{\rho_\tau}(\mathbf{x}, X^{\mathbb{T}} \setminus \mathcal{L}_t(\varphi_1)) = -\mathbf{dist}_{\rho_\tau}(\mathbf{x}, \mathcal{L}_t(\neg\varphi_1)) = -\mathbf{dist}_{\rho_\tau}(\mathbf{x}, \mathcal{L}_t(\varphi))$.

Case 3: $\varphi = \varphi_1 \vee \varphi_2$. By the induction hypothesis, for $i = 1, 2$,

$$-\mathbf{dist}_{\rho_\tau}(\mathbf{x}, \mathcal{L}_t(\varphi_i)) \leq [\![\varphi_i, \mathcal{O}]\!]_{\rho_\tau}(\mathbf{x}, t) \leq \mathbf{depth}_{\rho_\tau}(\mathbf{x}, \mathcal{L}_t(\varphi_i))$$

Implying

$$\sqcup_i -\mathbf{dist}_{\rho_\tau}(\mathbf{x}, \mathcal{L}_t(\varphi_i)) \leq \sqcup_i [\![\varphi_i, \mathcal{O}]\!]_{\rho_\tau}(\mathbf{x}, t) \leq \sqcup_i \mathbf{depth}_{\rho_\tau}(\mathbf{x}, \mathcal{L}_t(\varphi_i))$$

Now $\mathcal{L}_t(\varphi_1 \vee \varphi_2) = \mathcal{L}_t(\varphi_1) \cup \mathcal{L}_t(\varphi_2)$, therefore

$$\begin{aligned}
& \mathbf{depth}_{\rho_\tau}(\mathbf{x}, \mathcal{L}_t(\varphi)) \\
= \; & \mathbf{dist}_{\rho_\tau}(\mathbf{x}, (X^{\mathbb{T}} \setminus \mathcal{L}_t(\varphi_1)) \cap (X^{\mathbb{T}} \setminus \mathcal{L}_t(\varphi_2)) \\
\geq \; & \mathbf{dist}_{\rho_\tau}(\mathbf{x}, X^{\mathbb{T}} \setminus \mathcal{L}_t(\varphi_1)) \sqcup \mathbf{dist}_{\rho_\tau}(\mathbf{x}, X^{\mathbb{T}} \setminus \mathcal{L}_t(\varphi_2)) \\
\geq \; & [\![\varphi, \mathcal{O}]\!]_{\rho_\tau}(\mathbf{x}, t)
\end{aligned}$$

Similarly,

$$\begin{aligned}
-\mathbf{dist}_{\rho_\tau}(\mathbf{x}, \mathcal{L}_t(\varphi)) &= -[\mathbf{dist}_{\rho_\tau}(\mathbf{x}, \mathcal{L}_t(\varphi_1)) \sqcap \mathbf{dist}_{\rho_\tau}(\mathbf{x}, \mathcal{L}_t(\varphi_2))] \\
&= -\mathbf{dist}_{\rho_\tau}(\mathbf{x}, \mathcal{L}_t(\varphi_1)) \sqcup -\mathbf{dist}_{\rho_\tau}(\mathbf{x}, \mathcal{L}_t(\varphi_2)) \\
&\leq [\![\varphi, \mathcal{O}]\!]_{\rho_\tau}(\mathbf{x}, t)
\end{aligned}$$

Case 5: $\varphi = \varphi_1 \mathcal{U}_I \varphi_2$. $\mathbf{y} \in \mathcal{L}_t(\varphi) \Leftrightarrow \exists t' \in t +_R I$ s.t. $y \in \mathcal{L}_{t'}(\varphi_2)$ and $\mathbf{y} \in \mathcal{L}_{t''}(\varphi_1)$ for all $t < t'' < t'$
$\Leftrightarrow \exists t' \in t +_R I$ s.t. $y \in \mathcal{L}_{t'}(\varphi_2) \bigcap \cap_{t<t''<t'} \mathcal{L}_{t''}(\varphi_1)$
$\Leftrightarrow \mathbf{y} \in \cup_{t' \in t+_R I} [\mathcal{L}_{t'}(\varphi_2) \bigcap \cap_{t<t''<t'} \mathcal{L}_{t''}(\varphi_1)]$

Therefore $\mathbf{dist}_{\rho_\tau}(\mathbf{x}, \mathcal{L}_t(\varphi))$ equals

$$\begin{aligned}
& \mathbf{dist}_{\rho_\tau}(\mathbf{x}, \cup_{t' \in t+_R I} \left[\mathcal{L}_{t'}(\varphi_2) \bigcap \cap_{t<t''<t'} \mathcal{L}_{t''}(\varphi_1)\right]) \\
= \; & \inf_{t' \in t+_R I} \mathbf{dist}_{\rho_\tau}(\mathbf{x}, \mathcal{L}_{t'}(\varphi_2) \bigcap \cap_{t<t''<t'} \mathcal{L}_{t''}(\varphi_1)) \\
\geq \; & \inf_{t' \in t+_R I} \left[\mathbf{dist}_{\rho_\tau}(\mathbf{x}, \mathcal{L}_{t'}(\varphi_2)) \bigsqcup \mathbf{dist}_{\rho_\tau}(\mathbf{x}, \cap_{t<t''<t'} \mathcal{L}_{t''}(\varphi_1))\right] \\
\geq \; & \inf_{t' \in t+_R I} \left[\mathbf{dist}_{\rho_\tau}(\mathbf{x}, \mathcal{L}_{t'}(\varphi_2)) \bigsqcup \sup_{t<t''<t'} \mathbf{dist}_{\rho_\tau}(\mathbf{x}, \mathcal{L}_{t''}(\varphi_1))\right] \\
= \; & \inf_{t' \in t+_R I} \left[\mathbf{dist}_{\rho_\tau}(\mathbf{x}, \mathcal{L}_{t'}(\varphi_2)) \bigsqcup - \inf_{t<t''<t'} -\mathbf{dist}_{\rho_\tau}(\mathbf{x}, \mathcal{L}_{t''}(\varphi_1))\right] \\
= \; & \inf_{t' \in t+_R I} - \left[-\mathbf{dist}_{\rho_\tau}(\mathbf{x}, \mathcal{L}_{t'}(\varphi_2)) \bigsqcap \inf_{t<t''<t'} -\mathbf{dist}_{\rho_\tau}(\mathbf{x}, \mathcal{L}_{t''}(\varphi_1))\right] \\
= \; & - \sup_{t' \in t+_R I} \left[-\mathbf{dist}_{\rho_\tau}(\mathbf{x}, \mathcal{L}_{t'}(\varphi_2)) \bigsqcap \inf_{t<t''<t'} -\mathbf{dist}_{\rho_\tau}(\mathbf{x}, \mathcal{L}_{t''}(\varphi_1))\right]
\end{aligned}$$

PROOF SKETCH OF THM. IV.5

The proof of part 1 relies on the observation that $d_\tau(\mathbf{x}, \mathbf{y}, t) \leq |x_t - y_t|$, and using an induction on the structure of the formula. To show tightness, it suffices to provide a signal and formula where equality is achieved. For example, consider the one dimensional signal $\mathbf{x} \equiv 1, \mathcal{O}(p) = [0, \inf)$ and the formula $\varphi = \Box p$. Then it follows immediately that $|[\![\varphi, \mathcal{O}]\!]_{\rho_\tau}(\mathbf{x}, t)| = |[\![\varphi, \mathcal{O}]\!](\mathbf{x}, t)| = 1$. For part 2, the continuity of the signals ensures that as τ grows smaller, d_τ (Def. II.1) approaches the Euclidian distance, implying the rest.